

Article

New Adaptive Control Strategy for a Wind Turbine Permanent Magnet Synchronous Generator (PMSG)

Wenping Cao ¹, Ning Xing ^{2,*}, Yan Wen ^{1,*}, Xiangping Chen ^{3,*} and Dong Wang ^{4,*}

¹ School of Electrical Engineering and Automation, Anhui University, Hefei 230610, China; caowenping@hotmail.com

² College of Engineering and Applied Sciences, Aston University, Birmingham B4 7ET, UK

³ School of Electrical Engineering, Guizhou University, Guiyang 550025, China

⁴ Goldwind Science Technology Co. Ltd., Beijing 100176, China

* Correspondence: xingn@aston.ac.uk (N.X.); wenyanchn@gmail.com (Y.W.); ee.xpchen@gzu.edu.cn (X.C.); wangdong@goldwind.com.cn (D.W.)

Abstract: Wind energy conversion systems have become a key technology to harvest wind energy worldwide. In permanent magnet synchronous generator-based wind turbine systems, the rotor position is needed for variable speed control and it uses an encoder or a speed sensor. However, these sensors lead to some obstacles, such as additional weight and cost, increased noise, complexity and reliability issues. For these reasons, the development of new sensorless control methods has become critically important for wind turbine generators. This paper aims to develop a new sensorless and adaptive control method for a surface-mounted permanent magnet synchronous generator. The proposed method includes a new model reference adaptive system, which is used to estimate the rotor position and speed as an observer. Adaptive control is implemented in the pulse-width modulated current source converter. In the conventional model reference adaptive system, the proportional-integral controller is used in the adaptation mechanism. Moreover, the proportional-integral controller is generally tuned by the trial and error method, which is tedious and inaccurate. In contrast, the proposed method is based on model predictive control which eliminates the use of speed and position sensors and also improves the performance of model reference adaptive control systems. In this paper, the proposed predictive controller is modelled in MATLAB/SIMULINK and validated experimentally on a 6-kW wind turbine generator. Test results prove the effectiveness of the control strategy in terms of energy efficiency and dynamical adaptation to the wind turbine operational conditions. The experimental results also show that the control method has good dynamic response to parameter variations and external disturbances. Therefore, the developed technique will help increase the uptake of permanent magnet synchronous generators and model predictive control methods in the wind power industry.

Keywords: current-source converter (CSC); model predictive control (MPC); pulse-width modulation (PWM); voltage source converter (VSC); model reference adaptive system (MRAS)



Citation: Cao, W.; Xing, N.; Wen, Y.; Chen, X.; Wang, D. New Adaptive Control Strategy for a Wind Turbine Permanent Magnet Synchronous Generator (PMSG). *Inventions* **2021**, *6*, 3. <https://doi.org/10.3390/inventions6010003>

Received: 24 November 2020

Accepted: 24 December 2020

Published: 28 December 2020

Publisher's Note: MDPI stays neutral with regard to jurisdictional claims in published maps and institutional affiliations.



Copyright: © 2020 by the authors. Licensee MDPI, Basel, Switzerland. This article is an open access article distributed under the terms and conditions of the Creative Commons Attribution (CC BY) license (<https://creativecommons.org/licenses/by/4.0/>).

1. Introduction

The technology of wind turbines has been improving significantly over the last three decades [1–4]. The wind energy systems installation has increased by 30% in the previous decade. In 2018, the wind power capacity worldwide had reached 597 gigawatts, which is equivalent to 6% of the global electricity demand [5]. However, wind energy is characterised with its intermittency and unpredictability. At the early stage of wind-generation systems, synchronous generators and squirrel-cage induction generators were used for power generation, where any power fluctuations from wind would transmit to the grid. With the improvement of the wind energy conversion system (WECS), doubly fed induction generators (DFIGs) and permanent magnet synchronous generators (PMSGs) have become dominating wind turbine technologies, especially for medium and large wind

turbines. Compared to DFIGs which contain the rotor circuit in the machine, PMSGs can eliminate the gearbox and slip rings and thus provide a direct drive option. Furthermore, PMSGs have higher efficiency and power density than any other machines. In order to connect the generator with the power grid, a voltage source converter (VSC) and a pulse-width modulated (PWM) current source converter (CSC) are generally used with advanced control methods [6,7]. It is proved [7] that the latter is easier to achieve the current control and four quadrant operations. Because the PWM-CSC has the capability of controlling the DC voltage and current independently, the dynamic response of the system is excellent. As a result, this research chooses the PWM-CSC as a basic control method for PMSGs.

When the vector control is used in permanent magnet synchronous machines (PMSMs), the speed and rotor position information is mandatory [8]. In order to estimate the related parameters, the measurement sensors are usually chosen for PMSM. However, these sensors are costly and intrusive. Meanwhile, the installation and maintenance of these sensors increase the complexity and cost [9]. Because of these, sensorless control methods have been developed for adaptive control purposes. In the sensorless control strategy, the speed and/or rotor position are estimated by an estimator, which is designed by utilising predictive algorithms. Ideally these algorithms need to have excellent efficiency, quick response and low cost. While the design of Kalman filters tends to be sophisticated; switching law design of sliding mode controllers is involved. In the literature, existing sensorless methods are inefficient at low speeds or standstill, and some strategies are uneconomical for wind power applications [10,11].

In the developing process of sensorless control techniques, the back electromotive force (EMF) estimation is a common method for PMSM control [12,13]. It is easy to calculate, and provides excellent performance at high speeds. However, a stumbling block is that the back-EMF is dependent on the rotor speed. That is, the back-EMF is very small at low speeds so that it is difficult to achieve the accurate estimation under this condition [14–18]. The first commonly used solution to this problem is to develop a separate start-up strategy. The second solution is to utilise another control method with rotor position and speed at the low-speed range. Once the value of back-EMF is large enough, the back-EMF method can resume in operation.

Reference [19] presents a sensorless method for a standalone wind energy conversion system to estimate the power coefficient as per actual wind speeds. This is based on the extended Kalman filter (EKF) estimator. It consists of two steps: a prediction step and a correction step. In the prediction step, both the state vector x_k and covariance matrix P_p are predicted by expressing the Jacobian $F(k)$. In the correction step, the gain matrix $H(k)$ is determined, and this step corrects the predicted state vector and covariance matrix. Through the use of the EKF estimator, the PMSG currents i_d , i_q and the angular speed ω_e can be estimated. The method in [19] builds on a database which can be used to observe the characterisation of the platform. Alternatively, virtual instruments can also provide a sensorless method for wind power adaptive control. Nonetheless, this requires a nonlinear model, implemented by using multilayer perceptron neural networks [20]. This demands for computational resources and basic parameters are still needed to be determined with accuracy.

2. Aims and Objectives

Model reference adaptive system (MRAS) is the most popular strategy for sensorless control nowadays because it can provide a more straightforward implementation and does not have too much computational burden. In the conventional MRAS, the proportional-integral (PI) controller is normally used in the adaptive model and the adaptation mechanism. However, the PI controller is usually tuned by the trial and error method, which is inaccurate and tedious.

Therefore, this work aims to develop a new model reference adaptive control system for PMSG wind turbines. There are three objectives: (i) It develops an improved model predictive control (MPC) system for PMSGs; (ii) it combines the dead-beat control concept

with the predictive MRAS observer for estimating the rotor position and speed; (iii) it designs a new robust feature to tune the control parameters and to resist external disturbances by combining a back-EMF with an I-F control method. The control method is tested in simulation and experiments to validate its effectiveness.

Among the control systems, MPC systems have attracted much attention. The leading theory is that it predicts future states based on the system model in every possible control action. The best control action is chosen to minimise the cost function. MPC features with real-time online scrolling optimisation. The algorithm has multi-criteria requirements, and it is relatively simple to implement in the microprocessor. However, it usually requires a larger amount of computation than classical control schemes [21,22]. But tuning parameters is a problem during the control process. When the system parameters change, the output results of the PI controller will degrade dramatically. In order to enhance the capability of resisting disturbances, a sensorless MPC control method for PMSM [23] is developed based on a first-order Euler method. Then, by combining a back-EMF with an I-F control method, a new single-loop MPC is proposed, which merges the current loop and speed loop. This method will simplify the control algorithm and the system structure.

3. Proposed Sensorless Control Algorithm

The WECS is a highly nonlinear and complex coupled system to convert kinetic energy into electricity [24]. Its powertrain includes a wind turbine, an electrical generator, the transmission system, several inverters and converters [25]. Figure 1 shows a diagram of a WECS, and Figure 2 presents an interconnection of a WECS. The option of generator for the WECS can be a DFIG, a PMSG or a caged induction generator. In this research, a PMSG is chosen because of its high power density and direct-drive option.

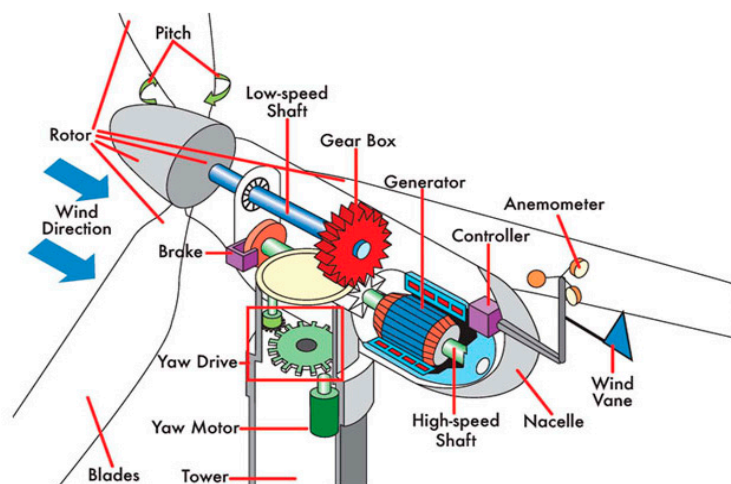


Figure 1. Components in a wind energy conversion systems [26].

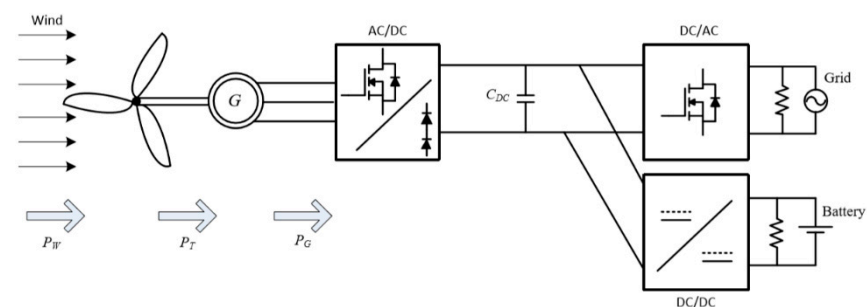


Figure 2. Illustration of interconnection of the wind energy conversion system (WECS).

The operational process of the WECS can be briefly summarised in three steps. The first step is to capture the mechanical aerodynamic energy from wind by the turbine blades. The second step is to convert the mechanical aerodynamic energy into the rotational mechanical one acting on the shaft of the generator. The third step is to convert this mechanical energy into electrical energy by the generator. In order to achieve the maximum power output from a wind turbine generation, a pulse-width modulated (PWM) converter is used to control the rotational speed of the generator as per the available wind energy. Through the generator-side converter and then grid-side inverter, the electrical energy is fed into the grid.

3.1. Configurations of PMSGs

Figure 3 shows three possible configurations for PMSGs. Figure 3a is a back-to-back configuration with two VSCs, which are efficient to manipulate the power flow in the system. As reactive power control is not required in PMSGs, and the diode rectifier can be used to reduce the cost. In order to maintain the DC link voltage and ensure the stability of the system, a DC/DC boost converter can be added between the rectifier and the VSC. This forms the second configuration, as shown in Figure 3b. Understandably, there is some extra cost and power loss in the boost converter. Figure 3c shows a PWM-CSC to integrate a PMSG with the power grid. In this configuration, a diode rectifier is used in place of a VSC and the inverter can control the power directly.

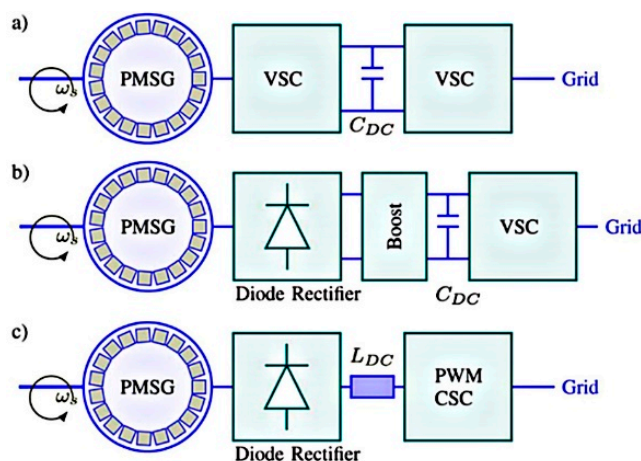


Figure 3. Three possible configurations for permanent magnet synchronous generators (PMSG) integration: (a) back-to-back converters with voltage source converters (VSCs). (b) Diode-bridge rectifier and boost converter. (c) pulse-width modulated-current source converter (PWM-CSC) [27].

Different to the VSC, the electrolytic capacitor is not needed in the PWM-CSC topology and thus reduces the size and cost [28]. Furthermore, the PWM-CSC has the short-circuit protection ability which gives a significant advantage [29].

Figure 4 further illustrates the structure of a PWM-CSC in the wind turbine generator system. When the wind speed is low and the EMF voltage of the machine reduces, the PWM-CSC directly controls the DC current, which significantly improves the efficiency of the system.

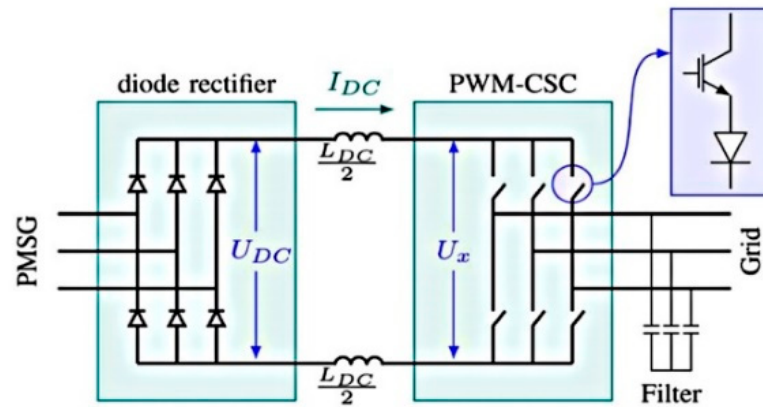


Figure 4. Schematic diagram of the conventional PWM-CSC.

3.2. The Proposed Sensorless and Adaptive Control Method

Based on the above analysis, a new sensorless and adaptive control method is developed. The schematic diagram of a PMSG wind turbine is shown in Figure 5.

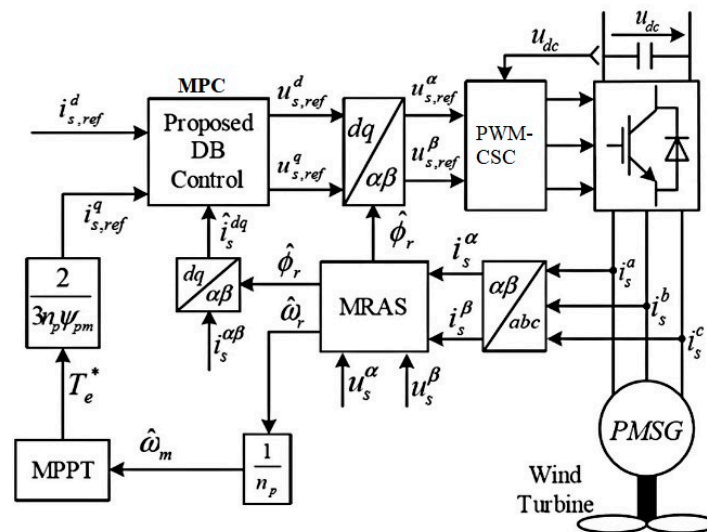


Figure 5. The schematic control diagram of a variable speed wind turbine PMSG.

The discrete-time model in the rotating d - q reference frame is given in Equation (1) [30,31]:

$$\begin{cases} u_s^d[k] = (R_{s0} + \Delta R_s)i_s^d[k] + (L_{s0} + \Delta L_s)\frac{i_s^d[k+1] - i_s^d[k]}{T_s} \\ \quad - (L_{s0} + \Delta L_s)\omega_r[k]i_s^q[k] + \varepsilon^d[k], \\ u_s^q[k] = (R_{s0} + \Delta R_s)i_s^q[k] + (L_{s0} + \Delta L_s)\frac{i_s^q[k+1] - i_s^q[k]}{T_s} \\ \quad + (L_{s0} + \Delta L_s)\omega_r[k]i_s^d[k] + \omega_r[k](\Psi_{pm0} + \Delta\Psi_{pm}) \\ \quad + \varepsilon^q[k], \end{cases} \quad (1)$$

where i_s^d , i_s^q , u_s^d and u_s^q are the d - q axis stator current and voltage of a PMSG, respectively. T_s is the sampling time; L_{s0} , R_{s0} and Ψ_{pm0} are the nominal values of the stator inductance, stator resistance and flux linkage, respectively.

In Equation (1), $\omega_r = n_p\omega_m$ which is the electrical angular speed of the rotor, n_p is the number of pole pairs and ω_m is the mechanical angular speed. $\varepsilon^d[k]$ and $\varepsilon^q[k]$ are the un-modelled d - q axis dynamics, respectively. ΔL_s , $\Delta\Psi_{pm}$ and ΔR_s represent the uncertainty of the stator inductance, PM flux linkage and stator inductance, respectively.

In different types of MPC approaches, the finite control set-model predictive control (FCS-MPC) and the deadbeat predictive (DB) control are two of the well-known methods. In this research, the DB control method is chosen. Although the FCS-MPC has received much attention because it is easy to implement, flexible to define control objectives and excellent in transient performance. Nevertheless, its disadvantages include the steady-state error, variable switching frequency and the need for a reference voltage. By using a space vector PWM (SVPWM), the reference voltage can be translated into the relevant switching actions [32]. But the system parameters are still necessary for the DB predictive control method.

In order to compensate for the unmodeled dynamics and make a piecewise constant variation, this work uses a discrete-time integral action (DTIA) in the DB algorithm. Upon the compensation action, an excellent steady-state response is obtained, and the robustness of DB predictive controller can be improved. The analytical relationship is as follows.

Assume R_{so} , Ψ_{pmo} and L_{so} are known constants. Because of the change in the frequency, temperature and load, ΔL_s , $\Delta \Psi_{pm}$ and ΔR_s are unknown. Meanwhile, they may change with time. In addition, the un-modelled dynamics $e^d[k]$, $e^q[k]$ are subjected to change with operating conditions. Thus, estimating these parameters with accuracy is technically challenging. By replacing $i_s^{dq}[k+1]$ with the reference value $i_{s,ref}^{dq}[k+1]$ in Equation (1) and adding the DTIA to Equation (2), the reference voltage $u_{s,ref}^{dq}$ can be calculated accordingly.

$$\begin{cases} u_{s,ref}^d[k] = R_{so}i_s^d[k] + L_{so} \frac{i_{s,ref}^d[k+1] - i_s^d(k)}{T_s} \\ \quad - L_{so}\omega_r[k]i_s^q[k] + k_I \sum_{n=0}^k e^d[n], \\ u_{s,ref}^q[k] = R_{so}i_s^q[k] + L_{so} \frac{i_{s,ref}^q[k+1] - i_s^q(k)}{T_s} \\ \quad - L_{so}\omega_r[k]i_s^d[k] + \omega_r[k]\Psi_{pmo} + k_I \sum_{n=0}^k e^q[n], \end{cases} \quad (2)$$

In Equation (2), $k_I \sum_{n=0}^k e^d[n]$ and $k_I \sum_{n=0}^k e^q[n]$ represent the DTIA removing the steady-state errors. These increase the robustness of the designed controller. When $k_I > 0$, the integral control gain and discrete-time current error are $e^d = i_{s,ref}^d - i_s^d$ and $e^q = i_{s,ref}^q - i_s^q$, respectively. If $k_I = 0$, the conventional DB algorithm will be simplified in the system.

In the proposed control strategy, the field-oriented control (FOC) method is applied, which has been widely used in synchronous and induction machines. In this method, the d -axis of the synchronous rotating reference frame aligns with the rotor flux. This alignment allows the magnetic flux and electromagnetic torque to be controlled independently, by controlling the d - and q -axis current components in the synchronous rotating reference frame, respectively. Different to the conventional MRAS, the PI controller in this work is replaced by the DB predictive controller to estimate the speed and rotor position of the PMSG.

4. Simulation Results

In order to study the proposed hybrid control method, a simulation model was first built within MATLAB/Simulink. The key parameters used in the simulation are listed in Table 1 and the detailed control scheme is presented in Figure 6 for illustration.

Simulation results are presented in Figures 7–12. Figure 7 shows the stator d - q voltages; Figure 8 shows the line to line voltage V_{ab} and Figure 9 shows the line current I_a . It can be seen that these electrical parameters can reach their steady-state and rated volages after a period of 0.15 s, which is three times of the electrical period. Figure 10 presents the electromagnetic torque; Figure 11 presents the speed tracking; and Figure 12 presents the active power output from the wind turbine generator. These are good performance

indicators to follow the expected references of the speed, torque and power. Despite slight overshooting in the first cycle, they can quickly arrive the rated values after approximately three cycles, which are similar to electrical parameters in Figures 7–9.

Table 1. Parameters of the PMSG wind turbine system [33].

Parameter	Value
Rated power P (W)	6000
Base power of the generator S (VA)	9444.44
Base wind turbine speed (m/s)	12
Rated speed ω (rad/s)	153
Stator resistance R (Ω)	0.425
No. of the pole pair	5
Rotor flux linkage (Wb)	0.433
Inertia J (kg m^2)	0.01197
Armature inductance L (H)	0.000395
Stator inductance L (H)	0.000835
Viscous damping F ($\text{N}\cdot\text{m}\cdot\text{s}$)	0.001189
The density of air ρ (kg m^3)	1.225
Area swept by blades A (m^2)	1.06

When setting $T = 1$ s in the simulation model, the active power waveform is obtained, as shown in Figure 12. From 0.02 s, the power starts to increase till 6123 W. Then, increasing T to 2, the power reaches 6120 W. When setting $T = 3$, the power reaches 6241 W. A comparison of results is given in Table 2 for the generator operating without an active control method, with MRAS and the proposed methods. It is shown that the PMSG using the proposed method can generate 3% more power than the conventional MRAS method, and 6% more power than that without employing an active method. A clear improvement of energy efficiency is demonstrated in this study.

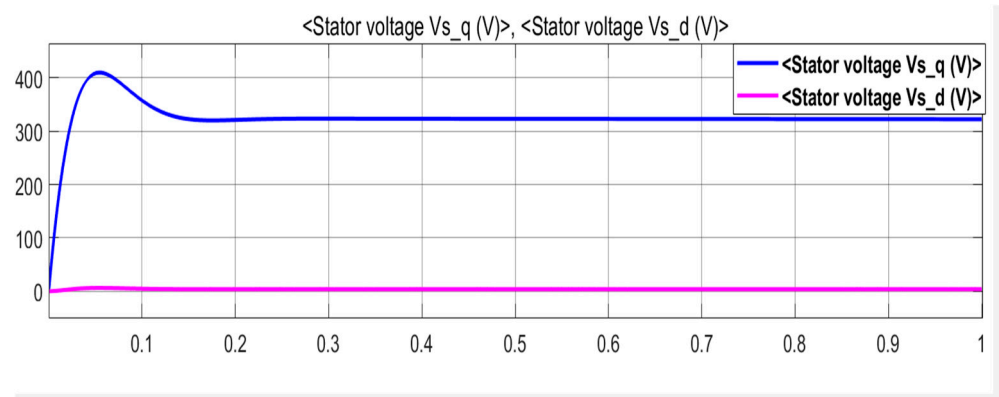


Figure 7. Stator d - q voltages.

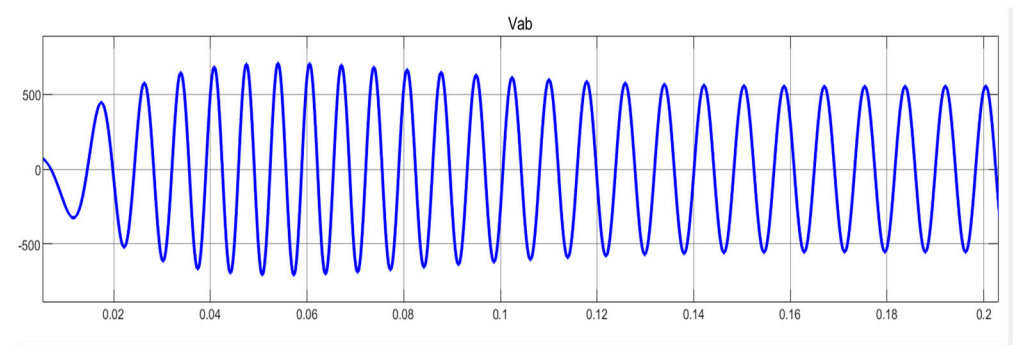


Figure 8. Line to line voltage V_{ab} .

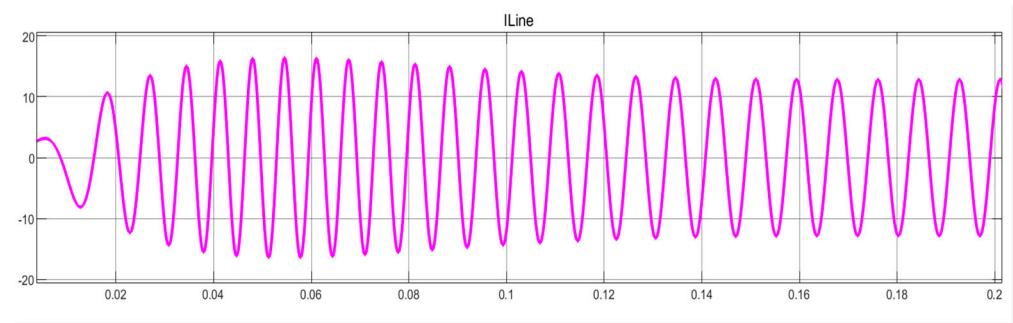


Figure 9. Line current I_a .

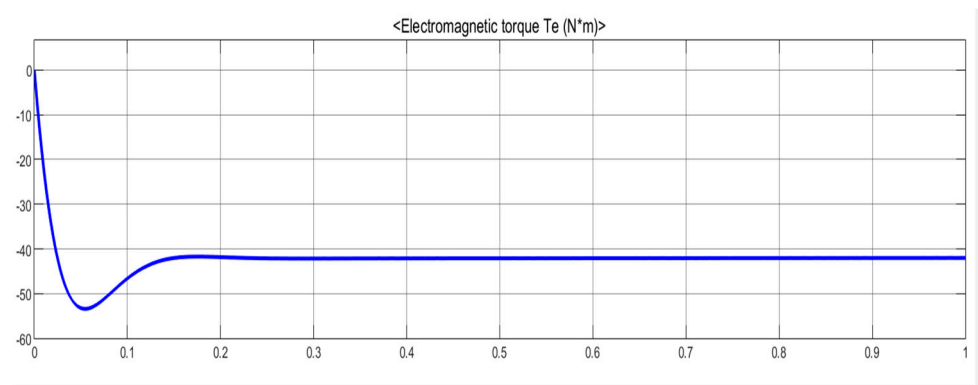


Figure 10. Electromagnetic torque.

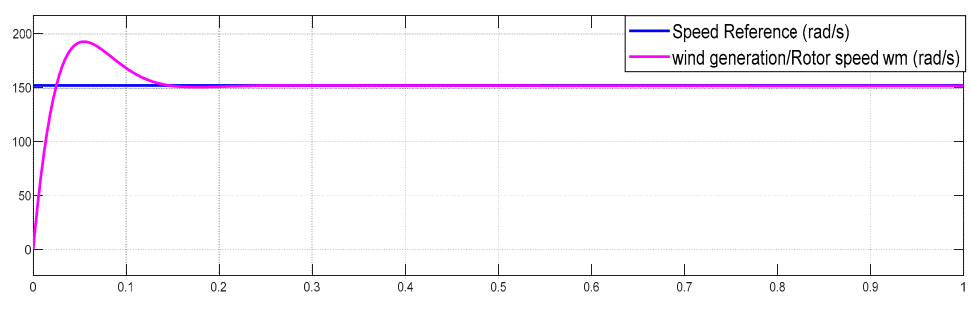


Figure 11. Speed tracking.

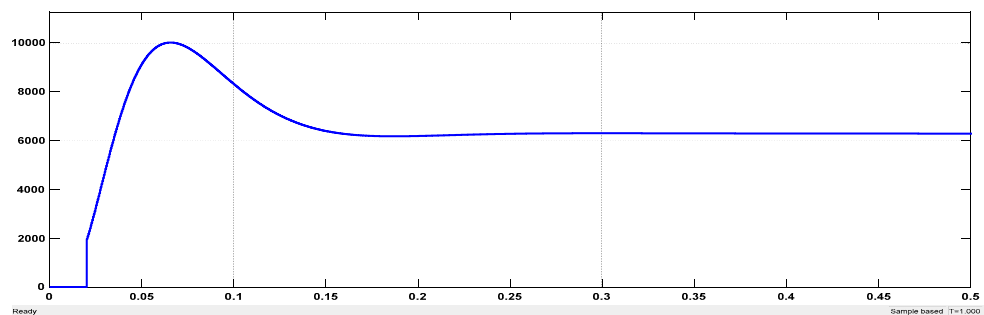


Figure 12. Active power output of the wind generator.

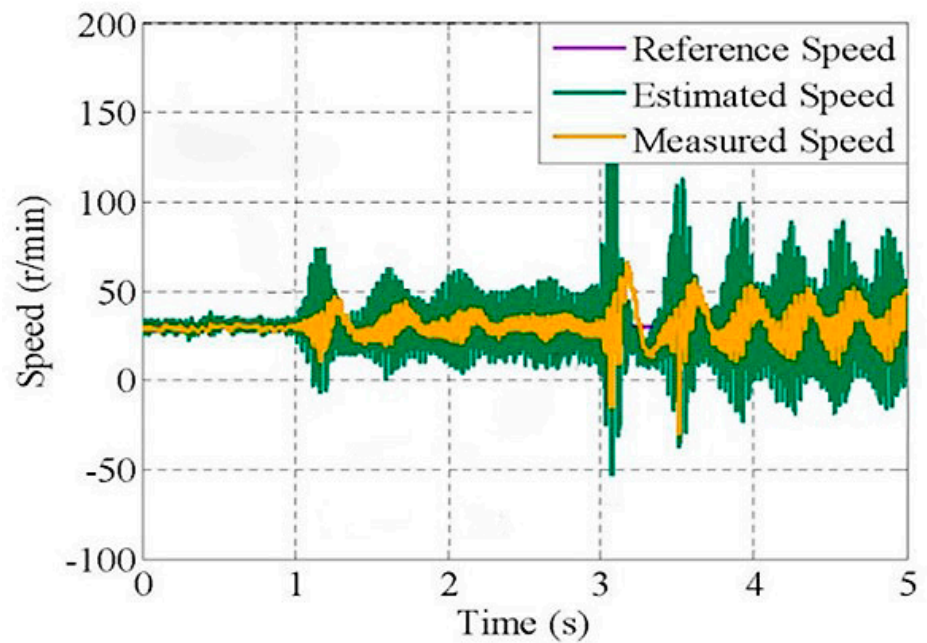
Table 2. Comparison of the output power using different control methods.

Types of Control Methods	$T = 1$	$T = 2$	$T = 3$
Without active control method	6143	6016	5974
MRAS control method	6132	6056	6078
Proposed MPC-MRAS method	6123	6120	6241

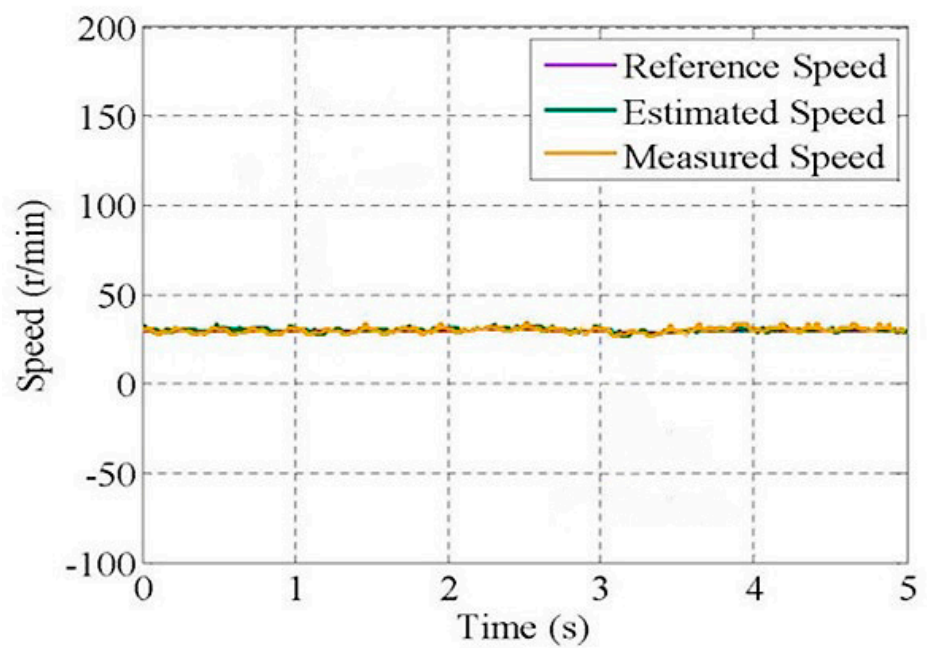
5. Experimental Results

In order to verify the effectiveness of the proposed method, an experimental test rig is set up. It consists of two EMJ-04APB22 servo motors, two High Voltage Motor Control and PFC Developer’s Kits (Texas Instruments). Among the two identical machines, they work back-to-back as a motor-generator (M-G) set, one acting as a motor to drive another working as a generator. The inverter switching frequency is 10 kHz. In the reference model, a low pass filter (LPF) is used to replace the integrator. The cut-off frequency of the LPF is set at 2 Hz.

The PMSG is tested under different loads and with different parameter variations to validate the effectiveness of the proposed MPC-MRAS method. As a comparison, the existing MRAS method is used as the benchmark. Some test results are shown in Figures 13–15.



(a)



(b)

Figure 13. Speed-tracking performance under the L_m change at no load. (a) model reference adaptive system (MRAS) control method. (b) Proposed model predictive control (MPC)-MRAS control method.

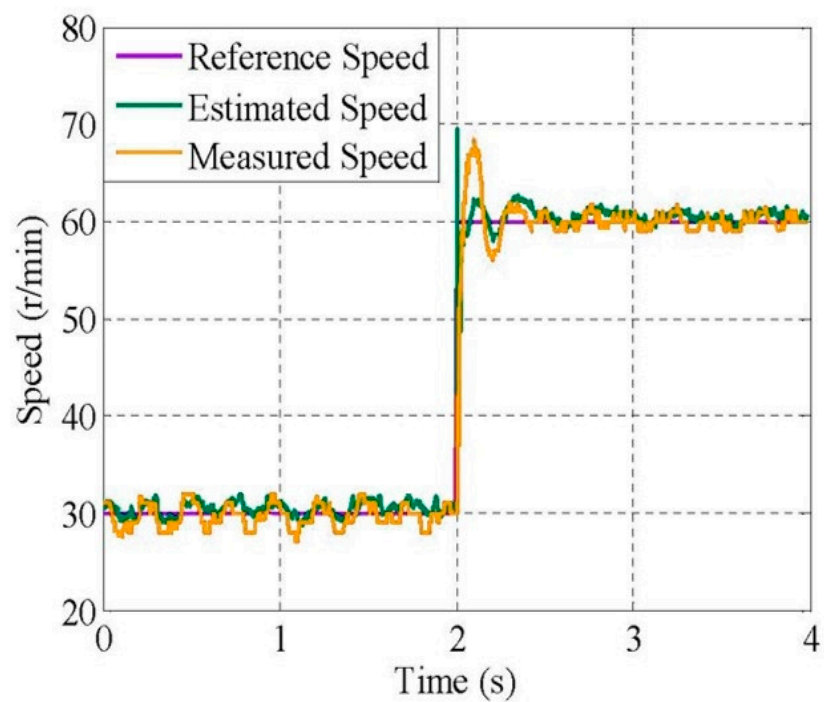
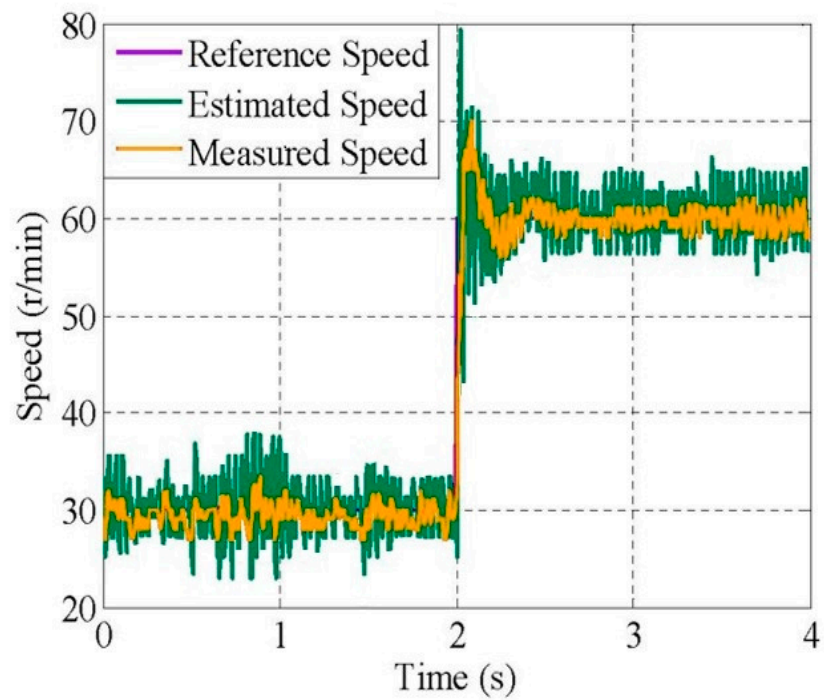
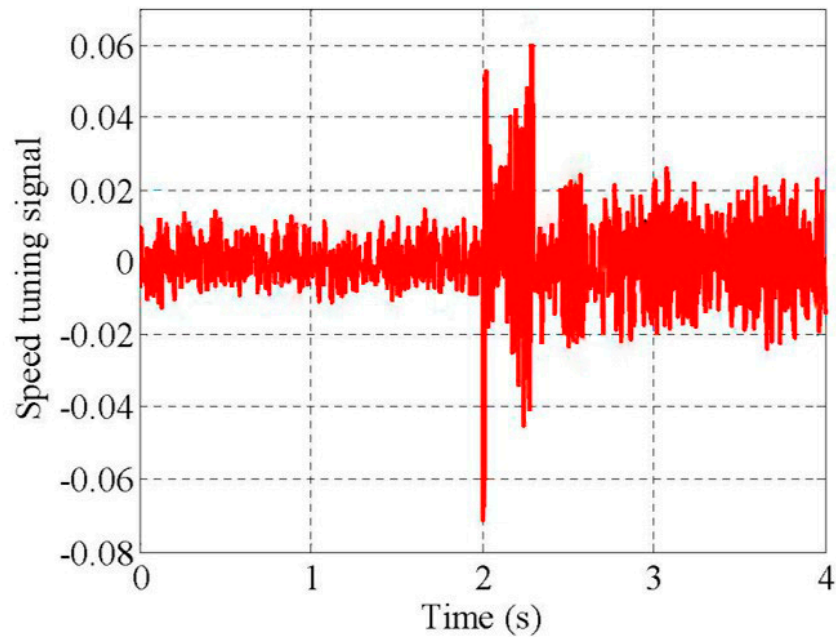
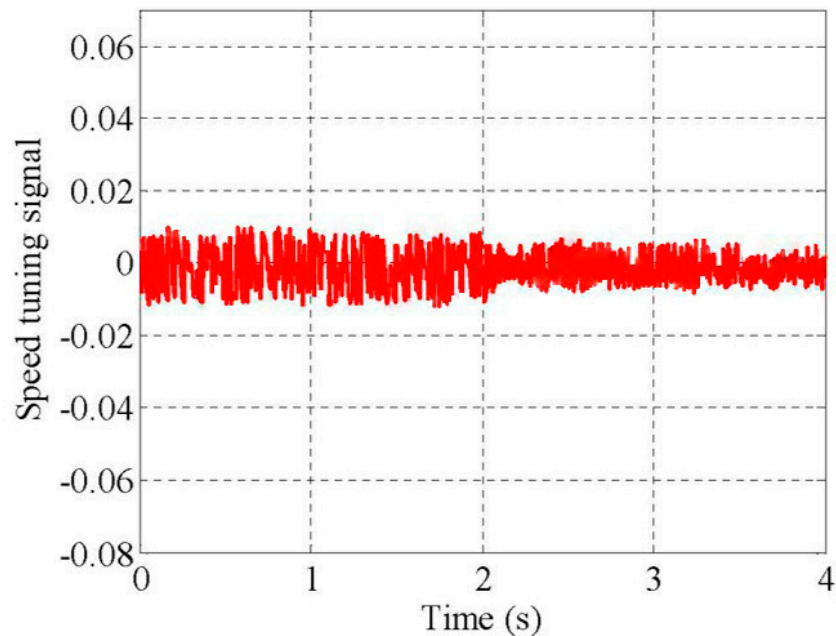


Figure 14. Speed-tracking performance under the reference speed change from 30 to 60 rpm at full load. (a) MRAS control method. (b) Proposed MPC-MRAS control method.



(a)



(b)

Figure 15. Speed-tuning signal under the reference speed change from 40 to 100 rpm at full load. (a) MRAS control method. (b) Proposed MPC-MRAS control method.

Figure 13 shows the PMSG's speed-tracking performance under the the mutual inductance change at no load. The estimation error is given by the difference between the measured parameter and estimated parameter. The accuracy of the control algorithms can be observed by comparing the similarities between the estimated parameters and the measured parameters lines in the figure. It is clear that the proposed MPC-MRAS control method can resist the disturbance from the L_m change whilst the conventional

MRAS method leads to significant fluctuations in the rotor speed. Moreover, the system stability has become an issue. Figure 14 presents the speed-tracking performance under the reference speed change from 30 to 60 rpm at full load. Upon a reference speed change, the PMSG with the proposed control method has reached a steady-state quickly and speed changes are low. On the contrary, the conventional MRAS presents continuous oscillations which are not dampened out after 5 s. Figure 15 demonstrates the speed-tuning signal under the reference speed change from 40 to 100 rpm at full load. After 2 s, the speed-tuning signal for the proposed control method remains at 0.012, but the speed tuning signal of conventional MRAS control method suddenly changed to 0.122 at 2 s. After then, it becomes very unstable. Clearly, the conventional MRAS gives rise to the fluctuations, which are as high as six times of that with the proposed method.

From experimental tests, Figures 13–15 demonstrate excellent robustness of the proposed MPC-MRAS control method as compared to the conventional MRAS control system.

6. Conclusions

This paper has presented a new sensorless and adaptive control method for variable speed control of a surface-mounted PMSG for wind turbine application. The use of a PWM-CSC helps operate the wind turbine under critical conditions. The proposed control method combines the dead-beat control concept with the predictive MRAS observer for estimating the rotor position and speed. Test results from simulation and experiments have confirmed that the proposed control system is effective and reliable. Compared to the existing methods, the proposed method provides better dynamic performance for PMSGs in wind turbine applications. Therefore, this control scheme has great potential to improve the dynamics and efficiency of wind turbine generators, thus promoting the uptake of PMSGs in the wind power industry.

However, in this work, the proposed control method has been tested on low-power PMSMs, which are off-the-shelf general-purpose machines used as PMSGs. In the further work, the developed technology will be implemented and field tested in medium and large wind turbine generators provided by the industrial partner Goldwind. Moreover, new artificial intelligence (AI)-based maximum power point tracking (MPPT) algorithms will also be developed and included in the control scheme so as to maximise the yield of wind turbines.

Author Contributions: In this work, the conceptualisation is developed by W.C. and N.X.; methodology, N.X. and X.C.; software, Y.W.; validation, N.X. and D.W.; writing—original draft preparation, N.X.; writing—W.C. and X.C.; supervision, W.C. and D.W. All authors have read and agreed to the published version of the manuscript.

Funding: This research was funded by Goldwind grant number 2016144.

Data Availability Statement: Data available on request due to restrictions. The data presented in this study are available on request from the corresponding authors. The data are not publicly available due to commercial reasons.

Conflicts of Interest: The authors declare no conflict of interest.

References

1. Blaabjerg, F.; Chen, Z. Power electronics for modern wind turbines. *Synth. Lect. Power Electron.* **2006**, *1*, 1–68. [CrossRef]
2. Arshad, M.; O’Kelly, B.C. Offshore wind-turbine structures: A review. *Proc. Inst. Civ. Eng. Energy* **2013**, *166*, 139–152. [CrossRef]
3. Failla, G.; Arena, F. New perspectives in offshore wind energy. *Philos. Trans. R. Soc. A Math. Phys. Eng. Sci.* **2015**, *373*, 20140228. [CrossRef] [PubMed]
4. Arrambide, I.; Zubia, I.; Madariaga, A. Critical review of offshore wind turbine energy production and site potential assessment. *Electr. Power Syst. Res.* **2019**, *167*, 39–47. [CrossRef]
5. WWEA. Wind Power Capacity Worldwide Reaches 597 GW, 50, 1 GW Added in 2018. Available online: <https://wwindea.org/blog/2019/02/25/wind-power-capacity-worldwide-reaches-600-gw-539-gw-added-in-2018/> (accessed on 25 February 2019).
6. Dai, J. Current Source Converters for Megawatt Wind Energy Conversion Systems. Ph.D. Dissertation, Ryerson University, Toronto, ON, Canada, 2010.

7. Lang, Y.; Wu, B.; Zargari, N. A high-power current source converter based wind energy system. *IEEE Trans. Ind. Appl.* **2008**, *55*, 2786–2797.
8. Li, Y.; Zhu, H. Sensorless control of permanent magnet synchronous motor—A survey. In Proceedings of the 2008 IEEE Vehicle Power and Propulsion Conference (VPPC), Harbin, China, 3–5 September 2008.
9. Singh, S.; Anvari-Moghaddam, A. Sensor-based and sensorless vector control of PM synchronous motor drives: A comparative study. In Proceedings of the 2018 IEEE 4th Southern Power Electronics Conference (SPEC), Singapore, 10–13 December 2018; pp. 1–6.
10. Sun, Y.; Preindl, M.; Siropour, S.; Emadi, A. Unified wide-speed sensorless scheme using nonlinear optimization for IPMSM drives. *IEEE Trans. Power Electron.* **2017**, *32*, 6308–6322. [[CrossRef](#)]
11. Zhao, H.; Wang, Z.; Xu, Y. A new speed sensorless controller based on double observers for permanent-magnet synchronous motor. In Proceedings of the 2016 8th International Conference on Intelligent Human-Machine Systems and Cybernetics (IHMSC), Hangzhou, China, 27–28 August 2016; pp. 401–404.
12. Giri, F. (Ed.) *AC Electric Motors Control: Advanced Design Techniques and Applications*; John Wiley & Sons, Ltd.: Hoboken, NJ, USA, 2013.
13. Nahid-Mobarakeh, B.; Meibody-Tabar, F.; Sargos, F.-M. Back-EMF estimation based sensorless control of PMSM: Robustness with respect to measurement errors and inverter irregularities. In Proceedings of the Conference Record of the 2004 IEEE Industry Applications Conference, 2004. 39th IAS Annual Meeting, Seattle, WA, USA, 3–7 October 2004; pp. 1858–1865.
14. Hassan, M.A.; Mahgoub, O.; El Shafei, A. ANFIS based MRAS speed estimator for sensorless control of PMSM. In Proceedings of the 2013 Brazilian Power Electronics Conference, Gramado, Brazil, 27–31 October 2013; pp. 828–835.
15. Mishra, A.; Mahajan, V.; Agarwal, P.; Srivastava, S.P. MRAS based estimation of speed in sensorless PMSM drive. In Proceedings of the 2012 IEEE Fifth Power India Conference, Murthal, India, 19–22 December 2012; pp. 1–5.
16. Xiao, D.; Guan, D.Q.; Rahman, M.F.; Fletcher, J. Sliding mode observer combined with fundamental PWM excitation for sensorless control of IPMSM drive. In Proceedings of the IECON 2014—40th Annual Conference of the IEEE Industrial Electronics Society, Dallas, TX, USA, 29 October–1 November 2014; pp. 895–901.
17. An, L.; Franck, D.; Hameyer, K. Sensorless field oriented control using back-EMF and flux observer for a surface mounted permanent magnet synchronous motor. *Int. J. Appl. Electromagn. Mech.* **2014**, *45*, 845–850. [[CrossRef](#)]
18. Nagarajan, V.S.; Balaji, M.; Kamaraj, V. Back-emf-based sensorless field-oriented control of PMSM using neural-network-based controller with a start-up strategy. *Adv. Intell. Syst. Comput.* **2015**, *325*, 449–457.
19. Mesbahi, A.; Raihani, A.; Bouattane, O.; Saad, A.; Khafallah, M. Extended Kalman Filter for characterizing a wind energy conversion system based on variable speed permanent magnet synchronous generator. In Proceedings of the 2014 International Renewable and Sustainable Energy Conference (IRSEC), Ouarzazate, Morocco, 17–19 October 2014.
20. Fortuna, L.; Giannone, P.; Graziani, S.; Xibilia, M.G. Virtual instruments based on stacked neural networks to improve product quality monitoring in a refinery. In Proceedings of the 2005 IEEE Instrumentation and Measurement Technology Conference Proceedings, Ottawa, ON, Canada, 16–19 May 2006; pp. 95–101. [[CrossRef](#)]
21. Rodriguez, J.; Cortes, P. *Predictive Control of Power Converters and Electrical Drives*; Wiley—IEEE Press: New York, NY, USA, 2012; Volume 40.
22. Rodriguez, J.R.; Kazmierkowski, M.P.; Espinoza, J.R.; Zanchetta, P.; Abu-Rub, H.; Young, H.A.; Rojas, C.A. State of the art of finite control set model predictive control in power electronics. *IEEE Trans. Ind. Inform.* **2013**, *9*, 1003–1016. [[CrossRef](#)]
23. Gao, J.; Liu, J.; Gong, C. A high-efficiency PMSM sensorless control approach based on MPC controller. In Proceedings of the IECON 2018—44th Annual Conference of the IEEE Industrial Electronics Society, Washington, DC, USA, 21–23 October 2018; pp. 2171–2176. [[CrossRef](#)]
24. Funabashi, T. Chapter 1: Introduction. In *Integration of Distributed Energy Resources in Power Systems*; Academic Press: Cambridge, MA, USA, 2016; pp. 1–14.
25. Yamasu, V.; Wu, B. Predictive control of a three-level boost converter and an NPC inverter for high-power PMSG-based medium voltage wind energy conversion systems. *IEEE Trans. Power Electron.* **2014**, *29*, 5308–5322. [[CrossRef](#)]
26. WindML. How Do the Wind Turbines Work? Available online: <https://www.windml.org/how-do-the-wind-turbines-work/> (accessed on 22 April 2020).
27. Giraldo, E.; Garces, A. An adaptive control strategy for a wind energy conversion system based on PWM-CSC and PMSG. *IEEE Trans. Power Syst.* **2014**, *29*, 1446–1453. [[CrossRef](#)]
28. Yang, S.; Xiang, D.; Bryant, A.; Mawby, P.; Ran, L.; Tavner, P. Condition monitoring for device reliability in power electronic converters: A review. *IEEE Trans. Power Electron.* **2010**, *25*, 2734–2752. [[CrossRef](#)]
29. Bai, Z.; Zhang, Z.; Ruan, X. A natural soft-commutation PWM scheme for current source converter and its logic implementation. *IEEE Trans. Ind. Electron.* **2011**, *58*, 2772–2779. [[CrossRef](#)]
30. Abdelrahem, M.; Hackl, C.M.; Kennel, R. Simplified model predictive current control without mechanical sensors for variable-speed wind energy conversion systems. *Electr. Eng.* **2017**, *99*, 367–377. [[CrossRef](#)]
31. Abdelrahem, M.; Hackl, C.; Kennel, R. Sensorless control of doubly-fed induction generators in variable-speed wind turbine systems. In Proceedings of the 2015 International Conference on Clean Electrical Power (ICCEP), Taormina, Italy, 16–18 June 2015; pp. 406–413.

-
32. Morel, F.; Lin-Shi, X.; Retif, J.-M.; Allard, B.; Buttay, C. A comparative study of predictive current control schemes for a permanent-magnet synchronous machine drive. *IEEE Trans. Ind. Electron.* **2009**, *56*, 2715–2728. [[CrossRef](#)]
 33. Lopez-Ortiz, E.N.; Campos-Gaona, D.; Moreno-Goytia, E. Modelling of a wind turbine with permanent magnet synchronous generator. In Proceedings of the 2012 North American Power Symposium (NAPS), Champaign, IL, USA, 9–11 September 2012; pp. 1–6.